JOURNAL OF MATERIALS SCIENCE **38** (2003) 3813–3829

Stress corrosion cracking fracture mechanisms in rock bolts

E. GAMBOA, A. ATRENS
Division of Materials, The University of Queensland, Brisbane, QLD 4072, Australia
E-mail: e.gamboa@minmet.uq.edu.au; a.atrens@minmet.uq.edu.au

Rock bolts have failed by Stress Corrosion Cracking (SCC). This paper presents a detailed examination of the fracture surfaces in an attempt to understand the SCC fracture mechanism. The SCC fracture surfaces, studied using Scanning Electron Microscopy (SEM), contained the following different surfaces: Tearing Topography Surface (TTS), Corrugated Irregular Surface (CIS) and Micro Void Coalescence (MVC). TTS was characterised by a ridge pattern independent of the pearlite microstructure, but having a spacing only slightly coarser than the pearlite spacing. CIS was characterised as porous irregular corrugated surfaces joined by rough slopes. MVC found in the studied rock bolts was different to that in samples failed in a pure ductile manner. The MVC observed in rock bolts was more flat and regular than the pure MVC, being attributed to hydrogen embrittling the ductile material near the crack tip.

The interface between the different fracture surfaces revealed no evidence of a third mechanism involved in the transition between fracture mechanisms.

The microstructure had no effect on the diffusion of hydrogen nor on the fracture mechanisms.

The following SCC mechanism is consistent with the fracture surfaces. Hydrogen diffused into the material, reaching a critical concentration level. The thus embrittled material allowed a crack to propagate through the brittle region. The crack was arrested once it propagated outside the brittle region. Once the new crack was formed, corrosion reactions started producing hydrogen that diffused into the material once again.

1. Introduction

The principle of rock-bolting is illustrated in Fig. 1 [1]. Rock bolts provide reinforcement above mine openings such as roadways. The rock bolts are bonded into the rock strata keeping it together just like the steel in reinforced concrete. The rock bolts can be considered to provide a clamping action on the rock. For the strata to fail and collapse, the clamping action of the rockbolts has to be overcome. This requires considerably greater forces. The rock bolts thus maintain the load bearing capacity of the rock strata.

The chemical bolt is the most common rock bolt currently in use [1]. The modern system [1] provides a quick, easy and effective installation procedure, Fig. 1b. An appropriate hole is drilled (to the appropriate diameter and depth), the chemical cartridge(s) and bolt is introduced into the hole, the bolt is rotated, and simultaneously pushed through the chemical cartridge(s) to mix together the resin and catalyst. After completion of the hold time (to allow curing of the chemical anchor) the bolt is tightened to the appropriate load. The load is distributed to the surrounding rock by means of the base plate, Fig. 1c. The chemical anchor fixes the bolt into the rock strata. Depending on amount of the chemicals used, the anchor can be at the end of the bolt as shown in Fig. 1c or it can extend along the length of the bolt. The amount of load on the bolt can be measured using strain gauged test bolts. Such experience allows estimation of the actual service load from the amount of plastic deformation of the support plate.

Any failure of a rock bolt is a potential concern. SCC failures of rock bolts have been reported at a number of Australian mines. SCC may occur whenever a highly-stressed steel is in the presence of an aggressive environment. The stress corrosion cracks initiate and grow slowly. During this phase there may be no indication of any danger. Fast fracture occurs when the stress corrosion cracks reach a critical length, as determined by the applied stress and the fracture toughness of the steel. Reports indicate that the critical crack length can be of the order of only a few millimeters for rock bolts. The fast fracture is sudden and catastrophic.

Rock bolts failed during service by Stress Corrosion Cracking (SCC) have been described previously [2–5]. Rock bolt microstructure is fine pearlitic steel.

Previous work [3, 5] on SCC of rock bolts has shown that service failures can be duplicated in the laboratory using the Linearly Increasing Stress Test (LIST)

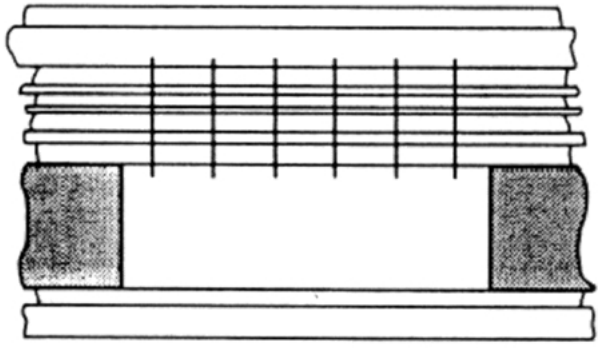

(a) Rock bolts provide reinforcement for rock strata above mine openings

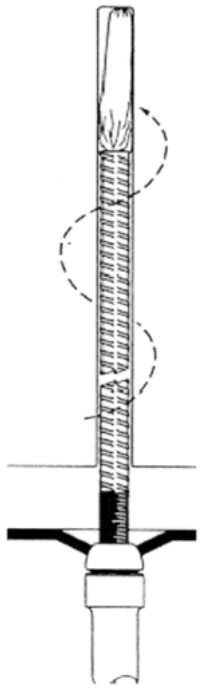

(b) The rock bolt is rotated, and at the same time pushed through the chemical cartridge mixing the resin components

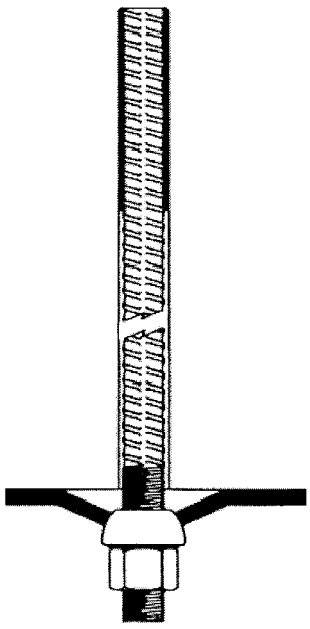

(c) A rock bolt after curing of the chemical fixative and tightening

Figure 1 Rock bolting.

apparatus [6]. LIST testing using a sulphate pH 2.1 solution at a rate of 0.019 $MPas^{-1}$ was found to provide a good foundation for a test to mimic service SCC. The resulting fractography of LIST samples were similar to those from service SCC [5].

The purpose of this work was to examine, in detail, the fracture surfaces in order to understand the fracture processes and to relate the fracture processes to the material microstructure. The fracture surfaces were related to work carried out by Toribio [4], in which the Tearing Topography Surface (TTS) has been documented. This paper compared the TTS documented by Toribio [4] to that found in rock bolts. A hypothesis was advanced regarding the crack propagation mechanism.

2. Experimental

Rock bolts were received from four Australian collieries. The bolts were photographed to record their macroscopic state (length, deformation due to shearing

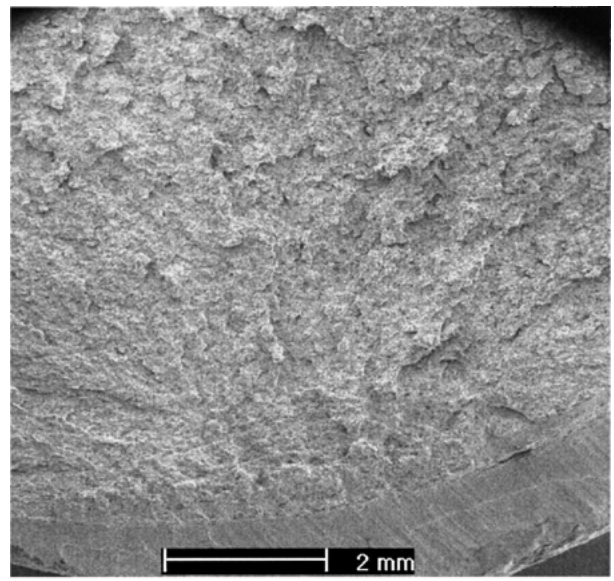

(a) SCC region overview

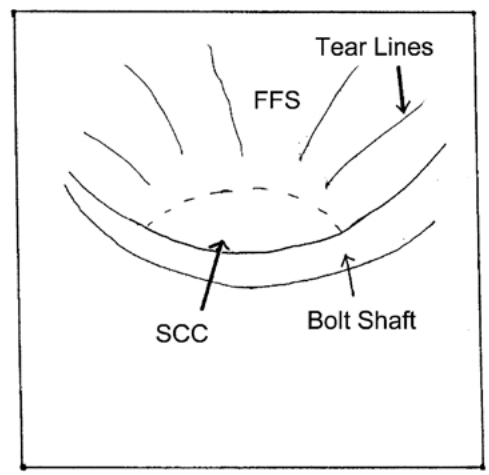

(b) Schematic view showing different fracture regions (FFS = Fast Fracture Surface)

Figure 2 SCC region overview.

in service, surface condition). Each fracture surface was prepared for SEM examination by cutting the bolt 10 mm from the fracture surface, and cleaning the fracture surface using 5% EDTA (Ethylenediaminetetra acetic acid disodium salt solution (EDTA)) to remove dirt and surface oxides. The cleaning period was kept to 2 min, as longer immersion times have a detrimental effect on the fracture surface. Normally only 30 to 60 s immersion was required to provide a good quality surface, but for high magnification work it was necessary to extend the immersion time. The cleaned bolt was mounted on an aluminium stub and observed with SEM.

3. Fracture surfaces

A convention used in the figures in this paper is that solid lines represent topographical features and dashed lines represent changes of fracture mechanism. Dot-dashed lines represent pearlite colony boundaries.

3.1. Overview

Fig. 2 illustrates a typical fracture surface of a bolt failed by SCC. The typical features were the thumbnail shaped slow crack growth region (SCC), surrounded by the fast brittle fracture region (Fast Fracture Surface (FFS) displaying cleavage fracture) marked by tear lines radiating out from the subcritical crack growth region. Crack branching was not evident on the slow crack growth region. On closer examination, SCC consisted of three distinct fracture morphologies: Tearing Topography Surface (TTS), Corrugated Irregular surface (CIS) and Micro Void Coalescence (MVC). TTS occurred close to the free surface whereas MVC was located mainly at the SCC-FFS transition. Most of the SCC region consisted of CIS.

3.2. Tearing topography surface (TTS)

The Tearing Topography Surface (TTS) occured close to the free surface. This topography has been described by Toribio and Vasseur [4] as a Tearing Topography Surface (TTS), a "*characteristic microscopic fracture mode with a kind of ductile tearing appearance, a certain degree of plasticity and a very closely spaced nucleation*" [4]. They point out that close to the surface of the specimen, the TTS has a kind of orientation in

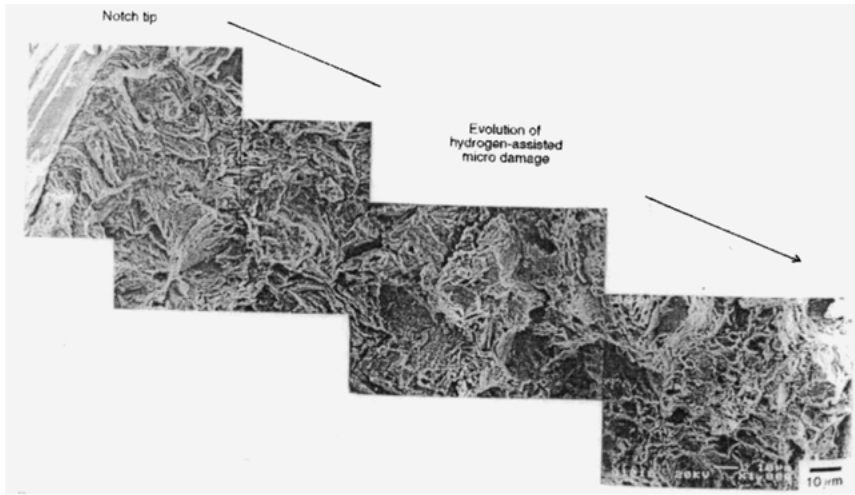

(a) Picture taken by Toribio and Vasseur of evolution of hydrogen assisted micro damage. [4]

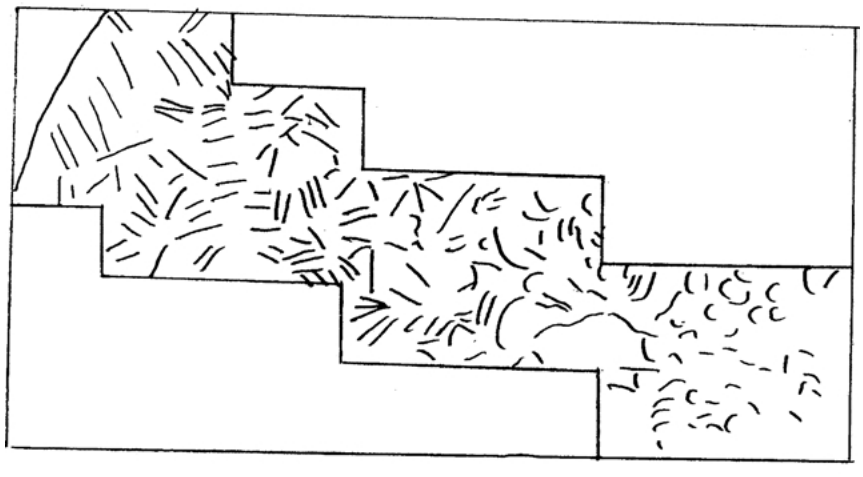

(b) Schematic view showing TTS ridge orientation

Figure 3 TTS region overview.

the direction of damage propagation. Such orientation was lost further into the sample. Fig. 3 shows such orientation. Close to the surface the deep ridges tended to point towards the free surface, but as the distance from the free surface increases, the orientation became random. Toribio [4] suggested that this fracture surface was formed by hydrogen diffused into the metal and assisting fracture by embrittling the material.

TTS occurred in rock bolt samples as shown in Figs 4 and 5. TTS in the rock bolts had a lower degree of orientation. Figs 4 and 5 illustrate the range of appearance for the TTS. These figures show the main features of TTS that were observed in rock bolts. These features are the flat ridged areas and the secondary cracks. The ridges sometimes seemed to radiate from one point within a flat area. At other places the ridges were parallel to each other. The flat regions within TTS did not correspond to a single pearlite grain as shown in Fig. 6. Fig. 6 shows also that the TTS ridged structure did not follow pearlite colony orientation nor pearlite colony boundaries, as pearlite colonies were aligned differently to the ridges. The flat region

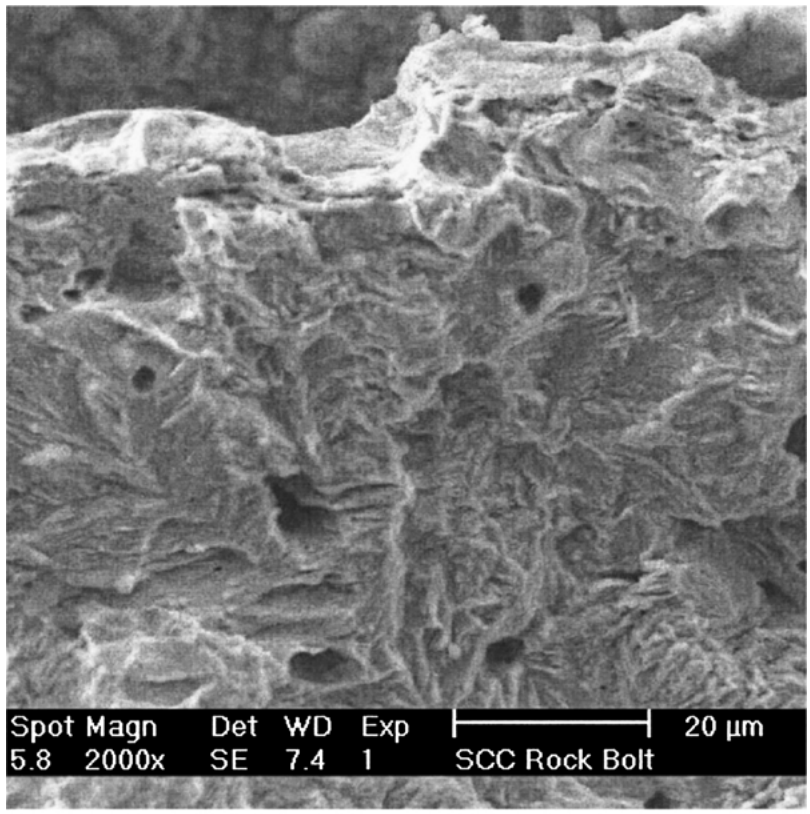

(a) Rock bolt TTS region.

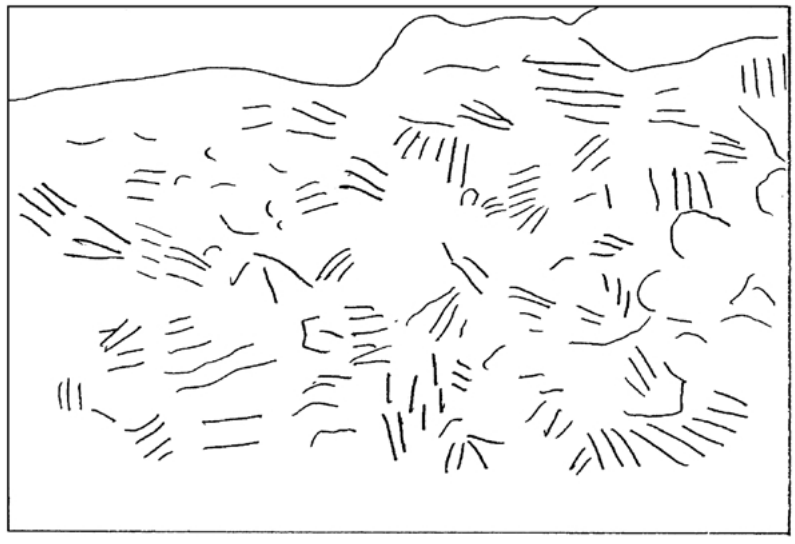

(b) Schematic view showing rock bolt TTS ridge orientation

Figure 4 Rock bolt TTS region.

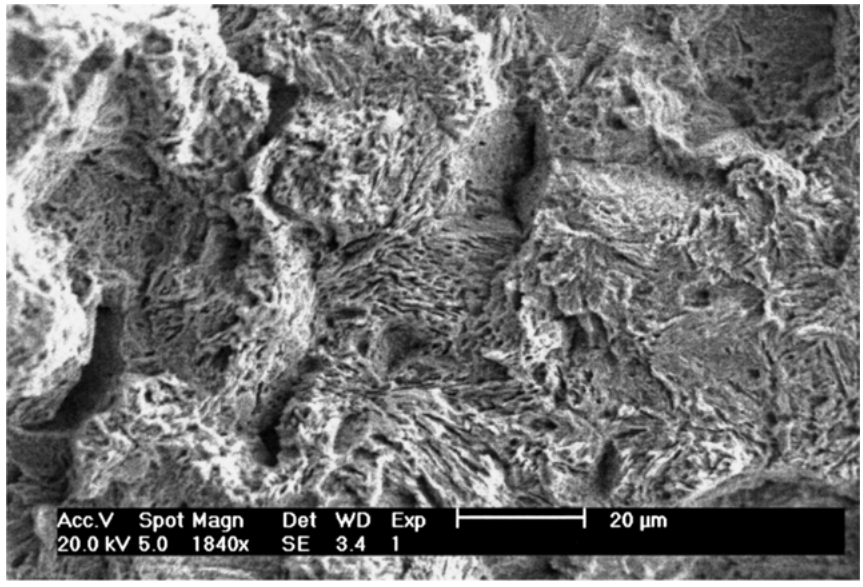

(a) Typical SCC close to free edge of sample (TTS)

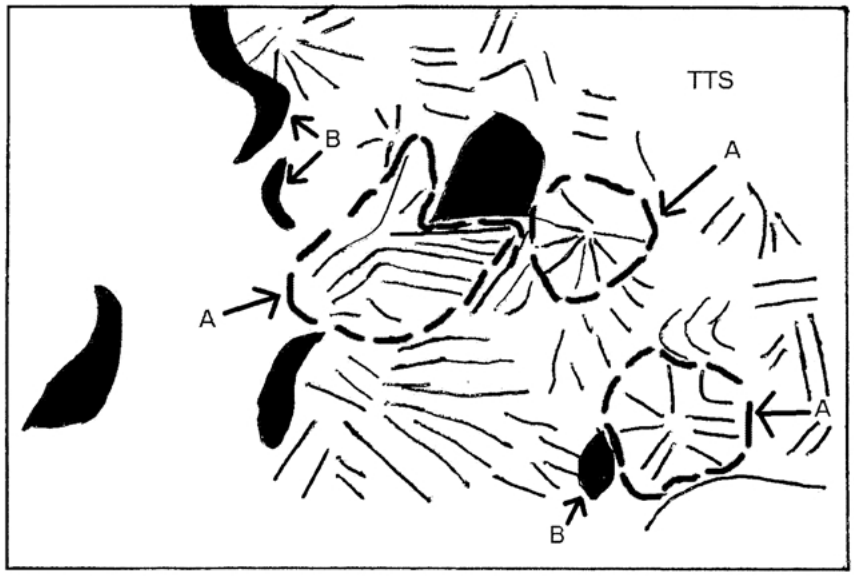

(b) Schematic view showing TTS. A: Flat region (bounded by dashed line) B: Chasm or secondary crack

Figure 5 Typical TTS.

shown by the figure was made up by at least 3 different pearlite colonies of different orientations (the dot-dash lines show the pearlite colony boundaries). Only the top colony followed the direction of the ridges, whereas the other two colonies were aligned perpendicularly to the ridge direction. The ridges of the top part of the figure had a spacing similar to the pearlite lamella, but the deep ridges apparent throughout the surface were not dependent on pearlite colony orientation; sometimes the pearlite colony lay perpendicular to these deep ridges. The perpendicular orientation of the ridges to the pearlite colony suggested that the fracture mechanism was independent of the pearlite.

3.3. Corrugated irregular surface (CIS)

The Corrugated Irregular Surface (CIS) [5] was characterised by porous irregular corrugated surfaces joined by rough slopes. The flat regions were perpendicular to the longitudinal axis of the rock bolt. Although there was a high quantity of slopes, there was overall a small change in depth in the fracture topography (of the order of a few hundred microns). Figs 7–8 show different aspects of CIS. CIS was typically found between the TTS and the Micro Void Coalescence (MVC) regions. In some cases, CIS was found at the edge of specimens instead of a TTS region.

Fig. 7 shows typical CIS regions. Fig. 7 also contains a diagram identifying the characteristic plateaus, slopes and isolated regions of Micro Void Coalescence (MVC). The holes in the surfaces of this figure was due to the cleaning process. This surface was cleaned with the EDTA solution for 15 min, before it was discovered that such a long immersion time introduced holes in the fracture surfaces although it produced no other discernible change. Subsequent

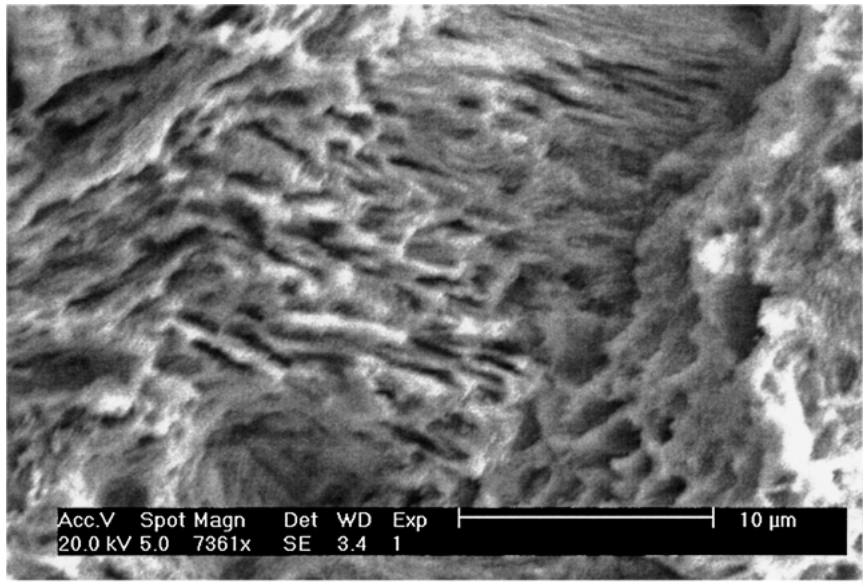

(a) Ridged structure of TTS

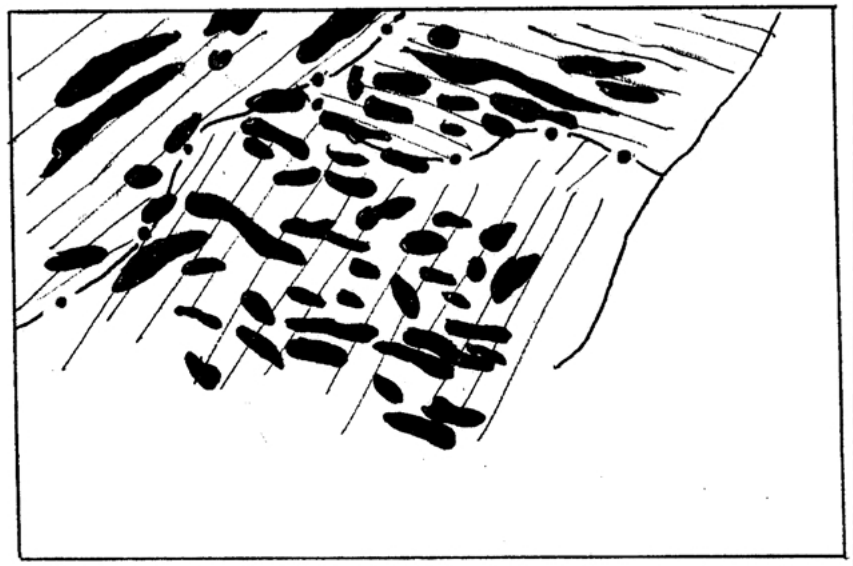

(b) Schematic view showing the ridge direction and pearlite colony orientation indicated by the fine parallel lines indicative of the direction of the plates of ferrite and carbide that make up the pearlite.

Figure 6 Higher magnification of Fig. 5.

surfaces have been cleaned for 2 min and rarely display holes.

Fig. 8 illustrates a plateau and the irregular corrugated slopes. In the foreground there was a plateau, with slopes leading down from the mesa in an irregular fashion. The mean change in depth between flat regions was of the order of 30 microns. Fig. 8 also shows the plateau at high magnification revealing the pearlite colonies and their orientation. The mean depth of features on these plateaus was of the order of a micron. The diagram depicts the different fracture regions, as well as the pearlite colony orientation.

The flat plateau regions within CIS were not individual pearlite grains. Fig. 8 shows that there were several pearlite colonies in each flat area, and that the boundary of such regions did not follow the orientation or the boundary of pearlite colonies.

3.4. Micro void coalescence (MVC)

Superficially, MVC found in samples failed by SCC appeared similar to that found in samples that had failed by ductile overload. On closer examination, SCC related MVC had subtle differences. Although dimple size could be similar, topographic height variations was different. In pure ductile overload samples, the fracture surface depth can vary of the order of 2 mm, whereas in SCC samples the depth change was of the order of 50 microns. Another difference was that SCC MVC could occur over relatively large flat regions with little change in height (of the order of 5 microns as seen on the top of Fig. 8).

An important point was that the bulk of the sample failure surface was cleavage (FFS), not MVC as in ductile overload samples. This suggested that the MVC region had been embrittled in some manner, suspectedly

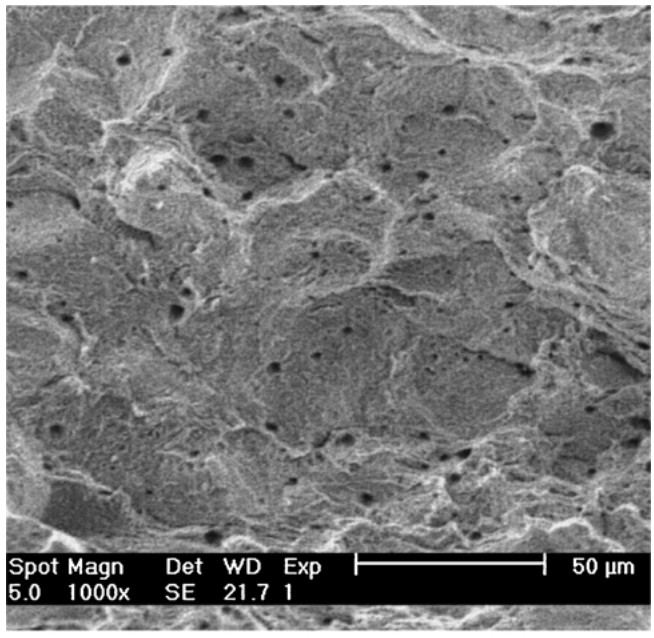

(a) Typical SCC (CIS)

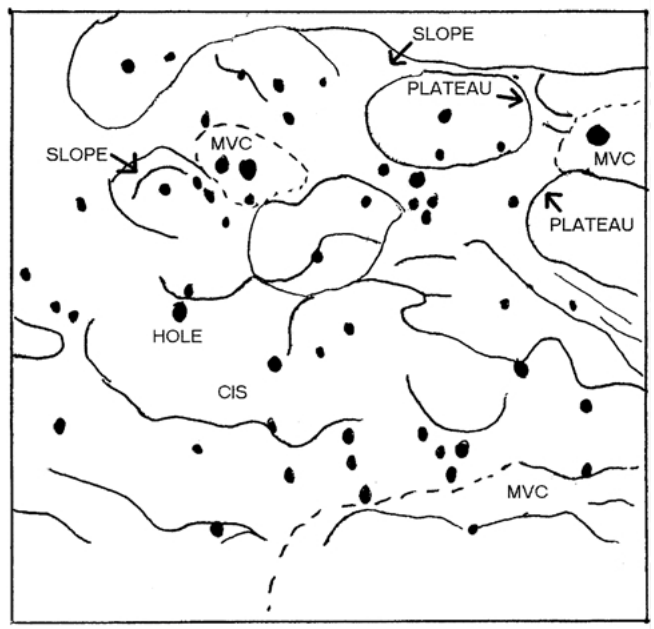

(b) Schematic view showing major features of SCC (CIS), including slopes and plateaus

Figure 7 Typical SCC (CIS).

due to hydrogen. It is believed that SCC MVC occured when the slow crack had achieved a critical size and the sample failed suddenly. Areas that had a significant concentration of hydrogen ahead of the crack tip did not fail by cleaving producing a FFS, but failed in an embrittled form of MVC. Toribio [4] mentions that "*With regard to the quasi-MVC topography, it appears only when the penetration path for the hydrogen is long compared with the dimensions of the sample . . . This seems to demonstrate that the MVC area is a "future" TTS zone which does not reach such a condition because of an insufficient level of hydrogenation.*" Toribio observed that the quasi-MVC region was found near the SCC-FFS transition. Similarly, MVC in this study was located mainly near the SCC (CIS)-FFS transition, although there were also pockets of MVC within the CIS regions.

4. Fracture surface interfaces

4.1. Interface TTS-CIS

The TTS-CIS interface was difficult to identify since both surfaces were similar in appearance. Both surfaces have small irregular, broken features. Usually they both showed a flat area with ridges upon its surface, while the surface did not show great topographical depth variance. Small pits could be found in either surface. The main differences between TTS and CIS was (1) the TTS surface was not as corrugated as CIS', and (2) the ridges tended to be more clearly defined in TTS. Slopes joining TTS flat regions were smaller, shorter and less common than CIS regions. The typical case was s TTS areas surrounded by CIS slopes. As the TTS had little orientation, the transition from one to the other fracture surface was difficult to pinpoint.

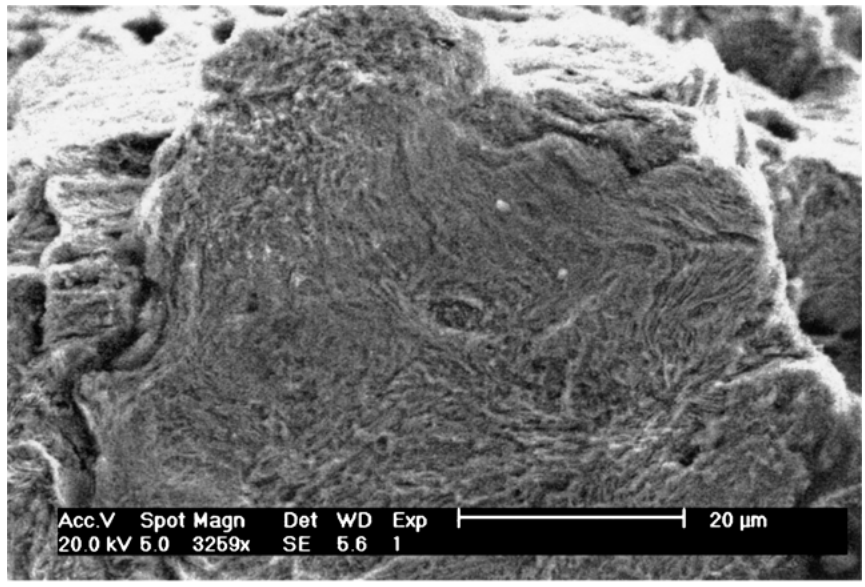

(a) CIS plateau showing pearlite colony orientation

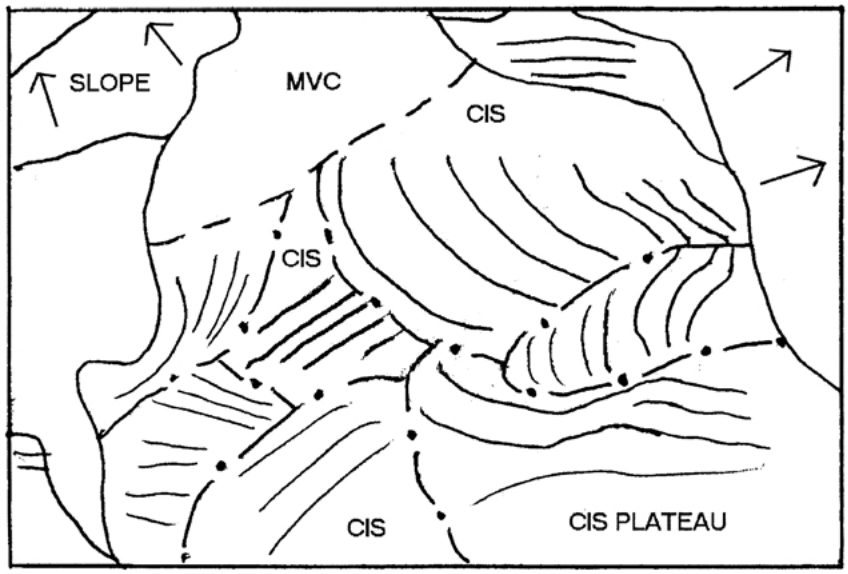

(b) Schematic view showing SCC (CIS) and MVC regions. Parallel lines show pearlite colony orientation. Arrows show down slopes.

Figure 8 High magnification view of a plateau within CIS.

4.2. Interface TTS-MVC, TTS-FFS

No cases have been found of a TTS region bordered with a MVC region, nor of TTS bordered with FFS. This indicated that TTS was associated with a high level of hydrogen, whereas MVC was associated with a low level. For the same reason it would be even less likely to find a pure TTS-FFS interface.

4.3. Interface CIS-MVC

The CIS-MVC interface was common. Fig. 9 shows one such interface. The MVC region was nestled between CIS and FFS. The topographical height difference between CIS and MVC could vary. At times MVC continued at the same height as CIS, with the interface line being difficult to identify. The sudden abundance of small microvoids was one way of identifying the change in these cases. This was the case in Fig. 9. The region in the MVC finger and in the lower right portion of the figure shows several small holes which were not readily found in the upper right portion (in the CIS region) of the figure. Fig. 14 shows one such hole in greater detail.

At other times, the CIS-MVC interface was clear as a steep CIS slope separated two fracture surfaces, one of which was a CIS plateau, while the other was the dimpled perforated MVC.

4.4. Interface CIS-FFS

On the left side of Fig. 9 was a typical CIS-FFS interface. The two surfaces were separated by a difference in height, joined by a steep corrugated slope. Cases have also been found where the fracture mechanism changed in the middle of a flat region.

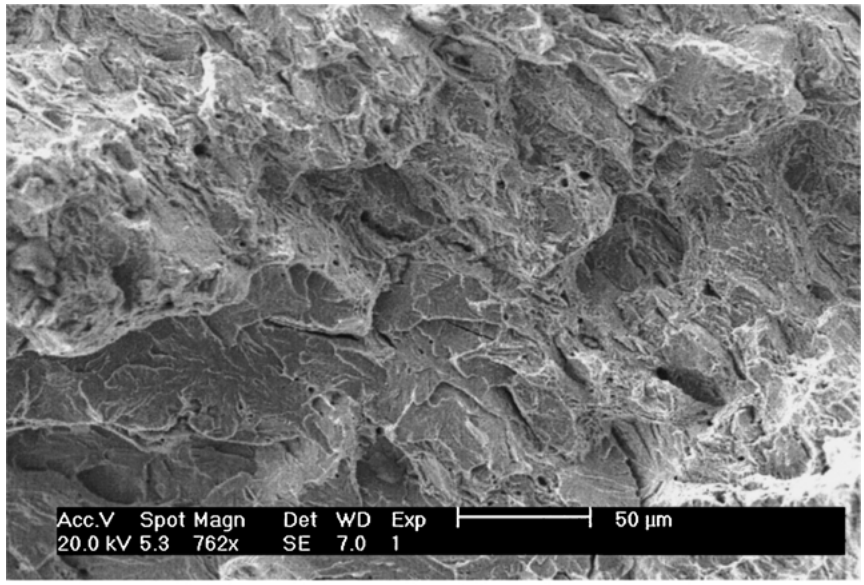

(a) SCC-MVC-FFS interface

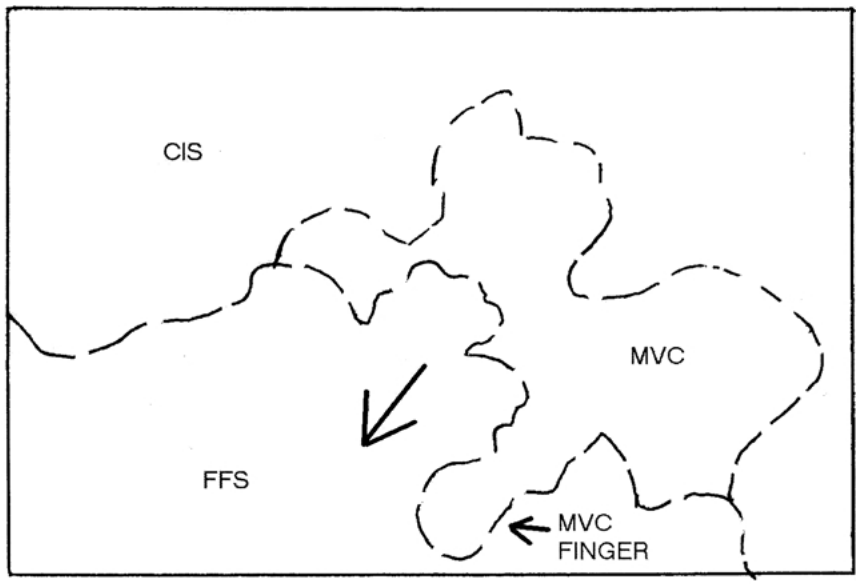

(b) Schematic view showing a MVC "finger" extending into the FFS. Large arrow shows crack growth direction.

Figure 9 Typical SCC-MVC-FFS interface.

Figs 10–12 show another case of the CIS-FFS interface. Fig. 10 shows CIS on the bottom part of the figure, with a slope leading down to the FFS region. The actual interface line was distinctive and has been indicated in the diagram. On one side of the line the surface was corrugated and irregular, while on the other side of the line the surface was flat and smooth. An interesting feature of this CIS-FFS interface illustrated in Fig. 10 were the "fingers" of CIS pointing inside the FFS. These "CIS" fingers were similar to the MVC fingers and are attributed to a similar mechanism.

Fig. 11 shows the pearlite colony orientation across the interface line. The diagram shows that the pearlite colony in the centre of the figure was aligned with the direction of the crack propagation. There was a clear imaginary line separating the coarse ridged area of the CIS and the smoother FFS. The pearlite colony lamella appeared coarser (grooves were more marked) in the CIS region, with the lamella of the same colony appearing smoother in the FFS region. This indicated that the fracture mechanism changed from CIS to cleavage in the middle of a pearlite colony in a very abrupt manner, indicating no third mechanism. At first sight it appeared that this coarser appearance of the lamella within the CIS region was due to preferential corrosion of one of the phases. This hypothesis was discarded as lamella near the free fracture surface would then be more markedly ridged as they would have been exposed to the electrolyte for longer periods of time, but this was not the case. The similarity of ridge depth at the interface and the free surface suggested that the coarseness was due to the fracture mechanism itself.

Fig. 12 shows the opposite. The diagram indicated that the pearlite colony direction towards the top of the

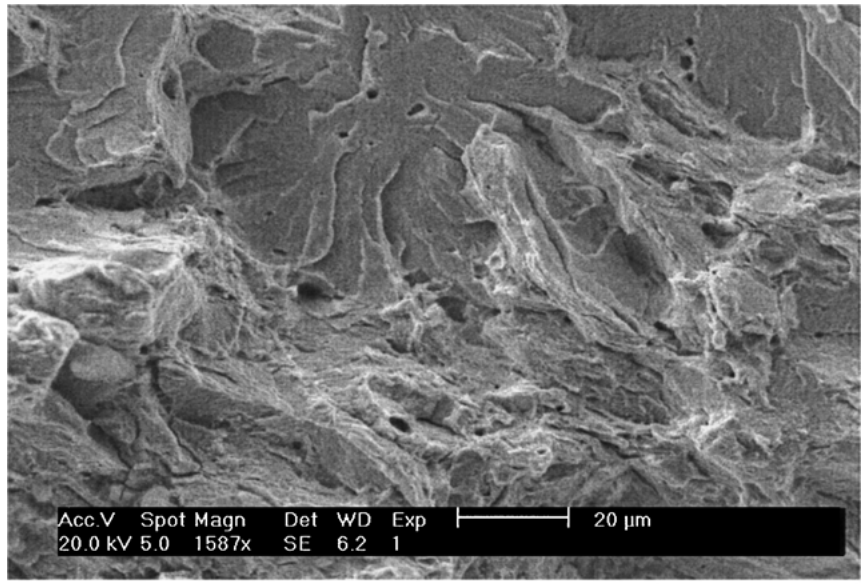

(a) CIS-FFS interface

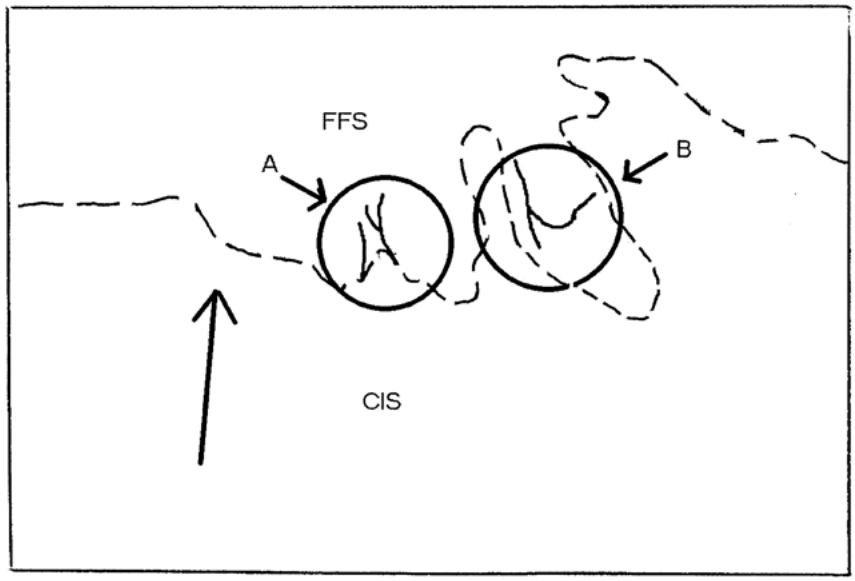

(b) Schematic view showing SCC(CIS) and FFS regions. Large arrow shows crack growth direction. A: Figure 11, B: Figure 12

Figure 10 Typical SCC(CIS)-FFS interface (x1587).

figure was perpendicular to the crack propagation direction. Towards the bottom of the figure the pearlite colony direction was not quite perpendicular to the crack propagation direction, but nevertheless it was at a high angle. The fracture mechanism changed from CIS to cleavage while the crack propagated perpendicular (or close to perpendicular) to pearlite lamella direction. Again a smooth transition suggested that there was no third fracture mechanism involved in the change over. Moreover, there was a change from CIS to FFS in the middle of a pearlite colony.

4.5. Interface MVC-FFS

The MVC-FFS interface was the most common one. Fig. 9 shows one typical interface. In the figure, the dimples were common near the interface, and holes are mostly restricted to the MVC side. The diagram shows that the interface line could waver. This suggested that the crack front grew in an irregular front rather than a straight uniform front. As the irregular crack front propagated, hydrogen propagated in front of the crack in a similar irregular manner giving rise to the irregular shape of the MVC region. The overall front could be macroscopically described as a straight line, as the average difference of penetration of the front into the FFS region was typically 50 microns.

Fig. 9 shows a MVC region that has grown as a "finger" into the FFS region, while the rest of the MVC-FFS interface was a relatively straight line. These fingers could extend into the FFS region by a much greater amount than the 50 microns mentioned previously.

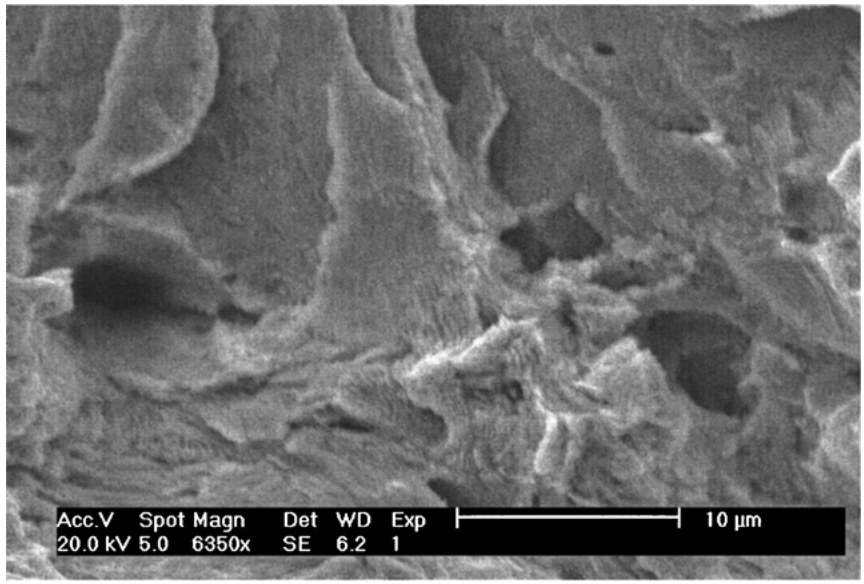

(a) SCC-FFS interface showing pearlite colony direction

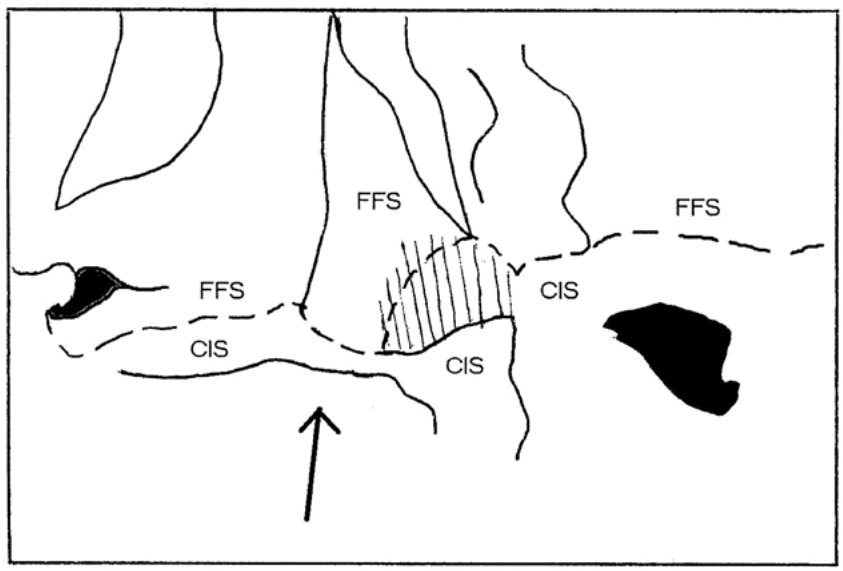

(b) Schematic view showing SCC(CIS) and FFS regions. Parallel lines show pearlite colony orientation. Large arrow shows crack growth direction.

Figure 11 Higher magnification view of region A of Fig. 10 (×6350).

Fingers have been detected of up to 350 microns in length, but tended to be a maximum of 100 microns across. These fingers are attributed to hydrogen finding a path that allows easier diffusion into the material.

Figs 13–15 show high magnification views of the MVC-FFS interface.

Fig. 13 shows the pearlite colony orientation across the interface. Fig. 13 also shows that the pearlite lamella was oriented parallel to the crack propagation direction and the interface was at an angle θ to that direction. The transition of MVC to FFS was smooth without a third mechanism. Fig. 14 shows an interface where the MVC side showed shallow dimples on a flat surface. There were several different pearlite colonies within this flat region, with different orientations. Fig. 15 shows another interface. This time pearlite colonies were aligned perpendicular to the crack direction, and the fracture mechanism changed within these perpendicular colonies. The change over was again smooth. Another point of note was that fast fracture tear lines were in close proximity to the interface line(as in Fig. 15). At times, these tear lines occurred within the same pearlite colony that displayed a change in fracture mechanism. Hence, the same colony with a single lamellar orientation could display a mechanism change as well as tear lines regardless of the pearlite orientation.

These Figures suggest that the pearlite colony orientation did not influence crack front direction nor fracture mechanism initiation. In other words, pearlite orientation did not affect hydrogen diffusion through the material.

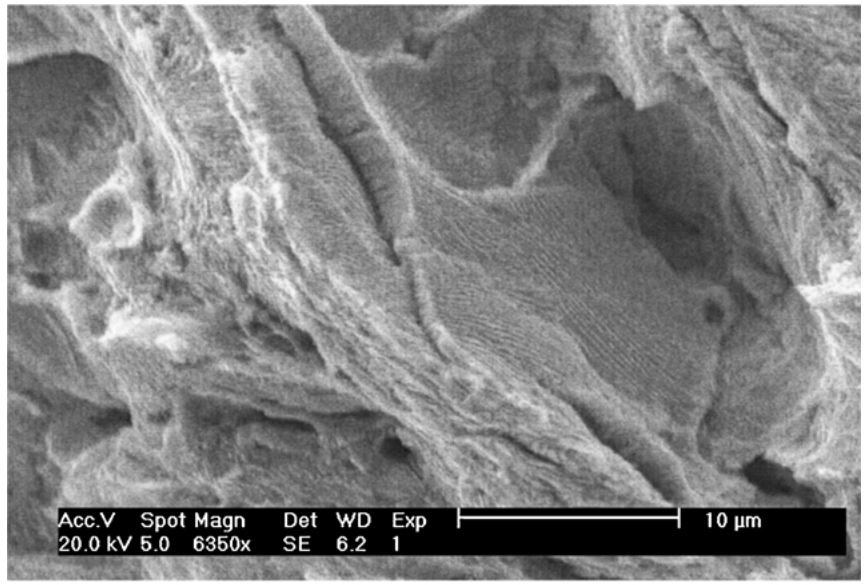

(a) SCC-FFS interface showing pearlite colony direction

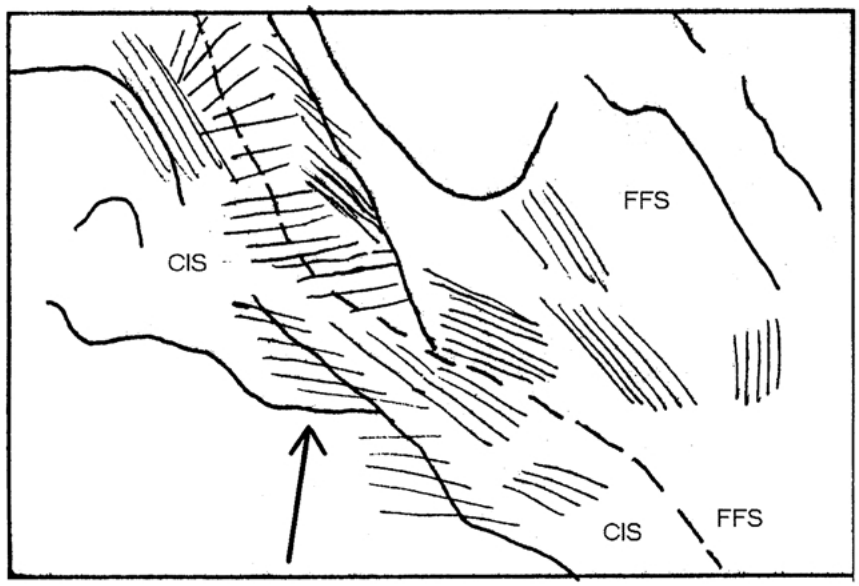

(b) Schematic view showing SCC(CIS) and MVC regions. Dashed line shows interface. Parallel lines show pearlite colony orientation.

Figure 12 Higher magnification view of region B of Fig. 10 (×6350).

5. Discussion

5.1. Macroscopic propagation

The random distribution of pearlite colony orientation within each fracture region (SCC (CIS), SCC (TTS) and FFS) suggested that the mechanism by which SCC propagates was not influenced at all by pearlite colony orientation. Furthermore, pearlite colony structure did not seem to influence the point at which the crack changes mechanism from slow subcritical crack growth to fast brittle propagation. Only fracture toughness of the material dictated the maximum crack size allowed before brittle failure.

The interface between SCC and FFS was created by the edges of the maple leaves appearing to be the transition line. The straightness of such a line suggested that the crack propagated as a front. Once the crack reached a critical size, the fast brittle failure occurred along the front at the same time. In many of those places, the crack propagated outward producing the maple leaf pattern. This resulted in the edges of the maple leaves creating a line along the crack front. In some cases, the separation between SCC and FFS was not so clear, as the transition region resembled a flat irregular dimpled surface (as in Fig. 14). This irregular dimpled surface was where hydrogen has had some time to diffuse ahead of the crack tip during the subcritical growth phase, enough to slightly embrittle the material. The resulting topography was similar to Micro Void Coalescence (MVC) found in ductile tearing. Hence the small region was neither pure ductile tearing nor brittle fracture.

The results suggested that as the corrosion reaction takes place during subcritical crack growth, released

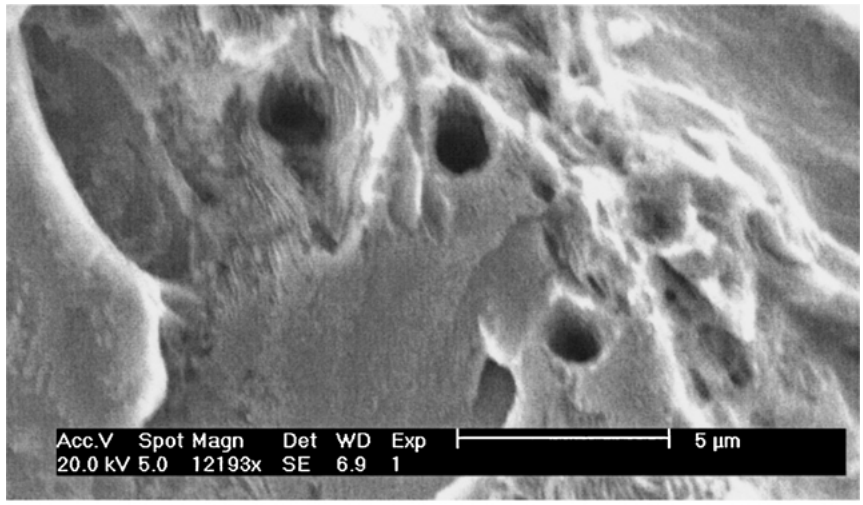

(a) MVC-FFS interface

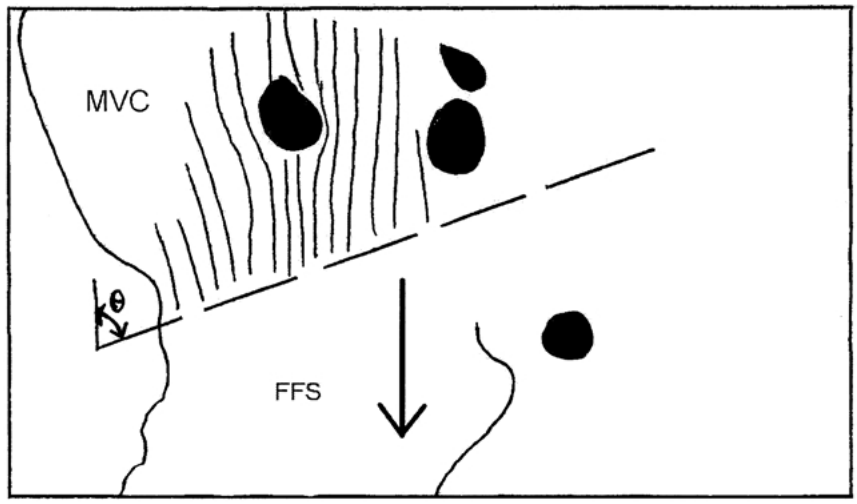

(b) Schematic view showing MVC and FFS regions. Parallel lines show pearlite colony orientation. Large arrow shows crack growth direction.

Figure 13 Typical MVC-FFS interface (×12193).

hydrogen at the crack tip diffused into the material irrespective of the metal microstructure. This was due to the size of hydrogen being several times smaller than other species of atoms, allowing the atoms to diffuse into the metal without difficulty. Hence due to triaxial stresses being higher perpendicular to the free surface of the material, hydrogen tended to diffuse ahead of the crack in greater concentration than parallel to the free surface. Such diffusion concentrated hydrogen to critical levels, whereupon the metal behaved in a brittle manner.

The resulting region of critical hydrogen concentration resembled the shape of a flame, as illustrated in Fig. 16. This shape was the result of two effects. The first effect was the diffusion of hydrogen into the material, driven by the concentration gradient and the triaxial stress at the crack tip. The region of hydrogen concentration due to the concentration gradient was a sphere around the crack tip, as shown in A. The second effect was due to the tensile stress present. The tensile stress (lower than the yield stress) caused the atomic bonds to stretch. Due to the stress concentration caused by the crack, the local stress at the crack tip was higher than inside the material, hence the atomic bonds at the crack tip were stretched elastically more than those further into the material. This is illustrated in B. As the bonds were stretched, the hydrogen atoms found an easier passage into the metal matrix than through the unstretched material. The resulting hydrogen concentration envelope is illustrated in C. By adding these two effects, the envelope of total hydrogen concentration is represented by D. Outside that envelope there still was hydrogen diffused into the material, but not to critical levels.

Once brittle, the crack propagated in a discrete step through the brittle region until it reached the hydrogen free ductile region, and the crack was arrested. The path the crack takes was random. Due to the high concentration of hydrogen just in front of the crack tip, the initial growth could occur in almost any direction. Due to the triaxial stresses there was a greater hydrogen concentration directly into the material, hence the crack grew directly into the material.

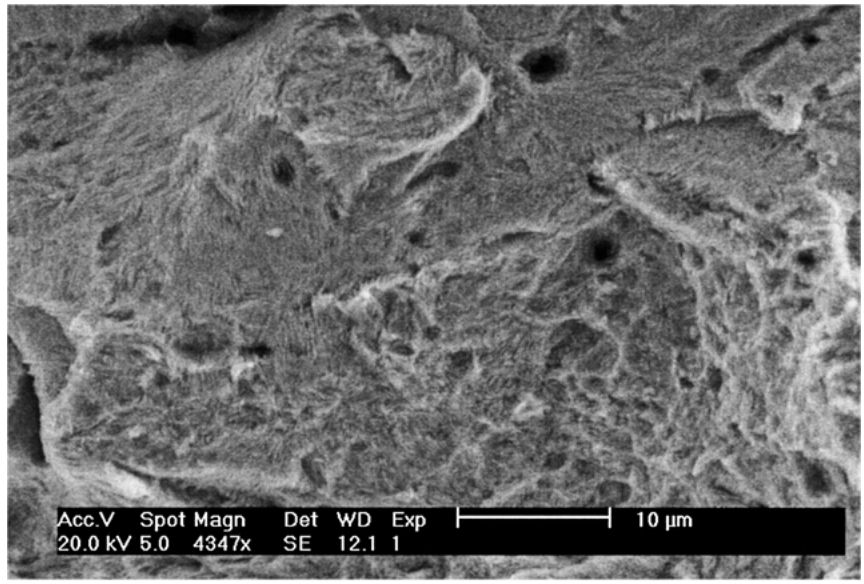

(a) High magnification image showing pearlite structure

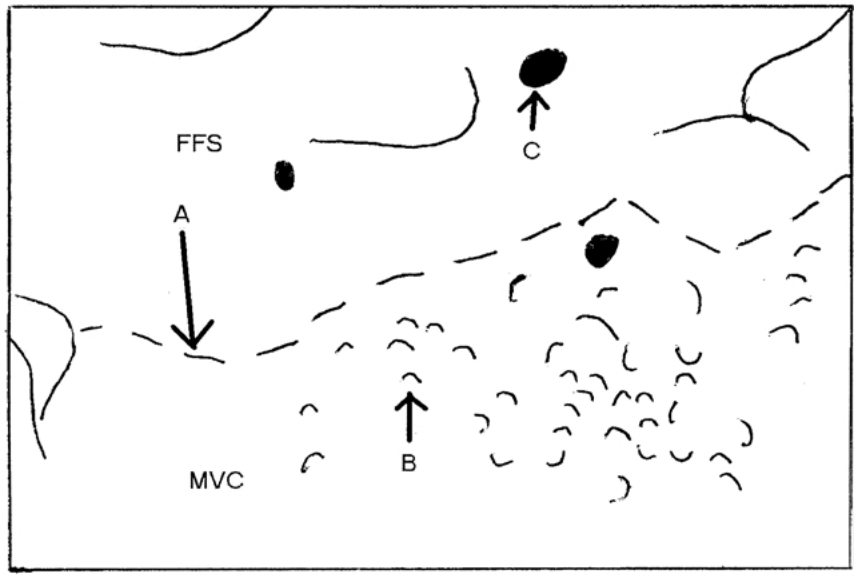

(b) A: Dashed line showing MVC-FFS interface, B: MVC dimples, C: Holes

Figure 14 Flat region within the SCC-FFS interface (×4347).

It is proposed that the slow crack growth mechanism can occur in two phases. The first phase consists of the crack growing in a random direction away from the free surface of the material. The crack could grow directly into the material, in a direction perpendicular to the applied stress. Overall, the SCC did indeed grow perpendicular to the applied stress. However, at the microscopic level, the crack could grow in any direction within the region of high hydrogen concentration. There were indeed many more possible directions at an angle to the perpendicular compared with the single possibility for crack growth directly ahead of the crack tip in a direction perpendicular to the applied stress.

A crack that did grow in a direction at a high angle to the perpendicular, eventually reached the region where the hydrogen concentration was insufficient to allow further propagation. At this point, it is suggested that there occurred the second phase of crack propagation.

The second phase consisted of the crack turning towards the perpendicular and growing into the material and growing in a direction where there was sufficient hydrogen concentration to support hydrogen assisted fracture. Hydrogen assisted fracture continued until the crack reached the ductile region in the material, where it was arrested. The corrosion process continued, with hydrogen entering the metal matrix and diffusing again ahead of the crack tip.

Fig. 17 presents the suggested mechanism for crack propagation within the embrittled region:

(a) The volume with the solid line stretching out from the crack was a region that had reached the critical

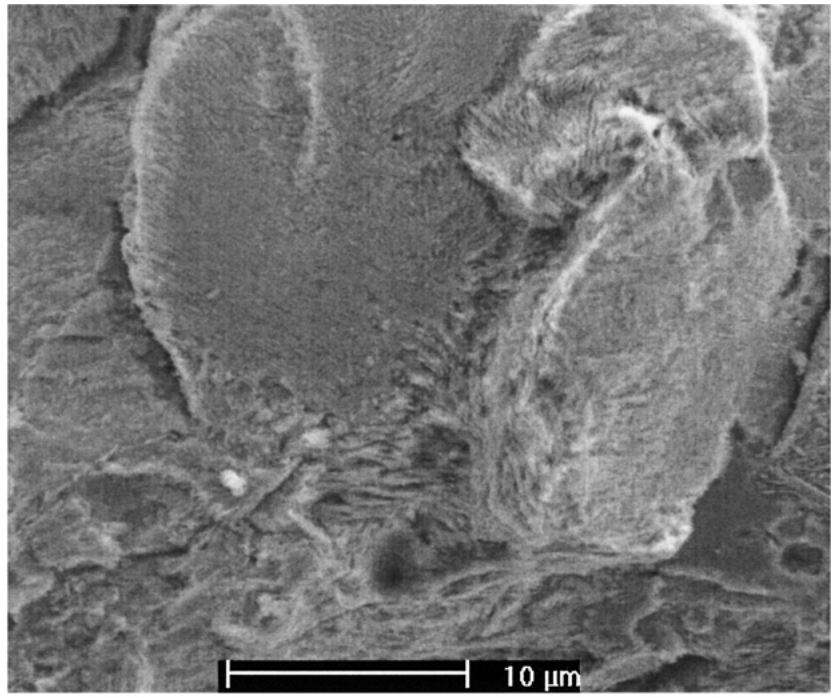

(a) High magnification image showing pearlite structure

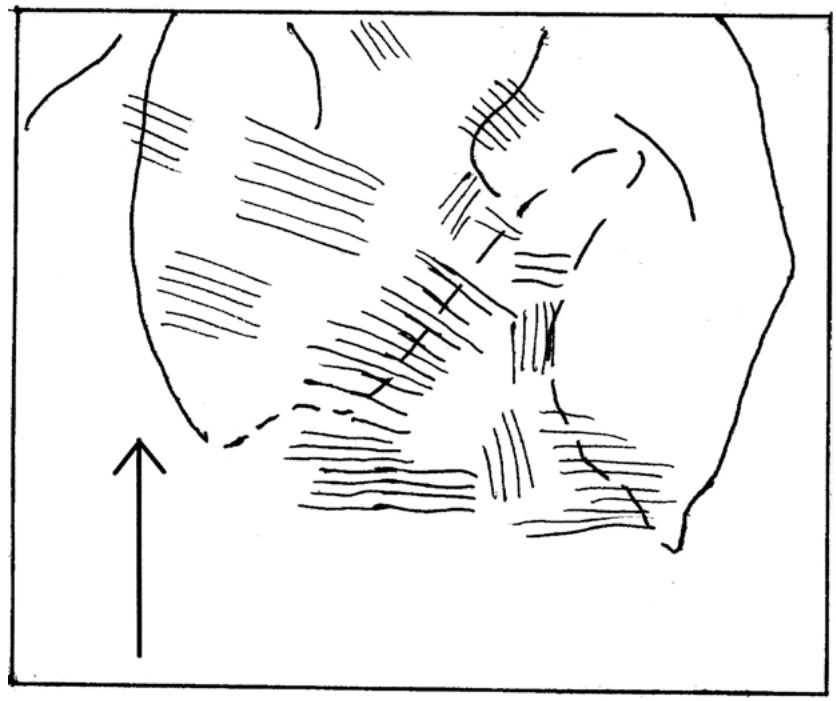

(b) Dotted line is the SCC-FFS interface. Parallel lines are pearlite colony orientations. Large arrow is crack growth direction.

Figure 15 SCC—fast fracture interface.

concentration of hydrogen; that region was now brittle. The volume between the dotted line and the solid line was a region that has some hydrogen but the hydrogen content had not yet reached a critical level.

(b) The crack propagated in a random direction with the tendency of staying within the brittle region. Crack propagation at a high angle away from the perpendicular corresponded to a CIS slope on the fracture surface. Overall the fracture surface was perpendicular to the applied stress. The CIS slopes made significant angles to this overall direction. This was because fracture surfaces were observed perpendicular to the fracture surface.

(c) The crack turned and grew directly into the material due to the tensile stress, aided by the larger embrittled region directly in front of the crack. The crack was arrested when it extended beyond the brittle region. This phase corresponded to a long flat region, hence a plateau. Due to the nature of the SEM it was difficult to determine the angle the plateau made to the

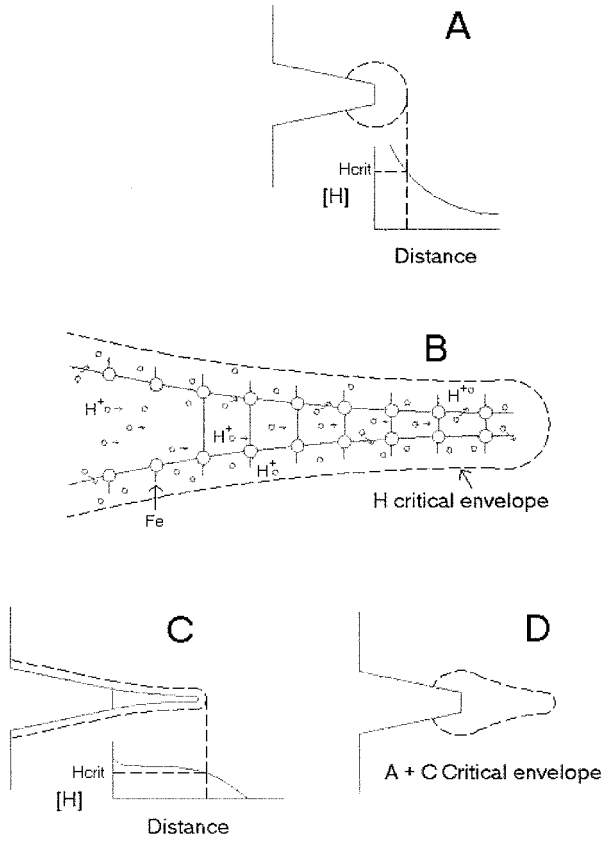

Figure 16 Critical hydrogen envelope.

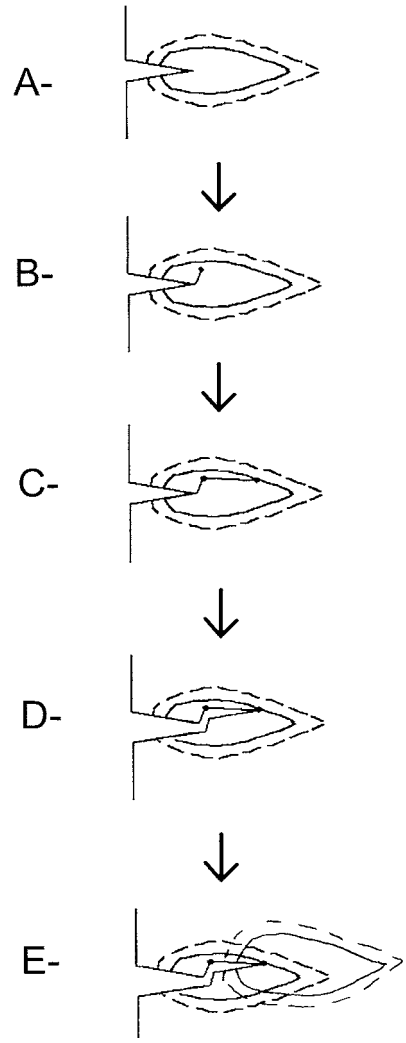

Figure 17 Slow crack growth propagation.

perpendicular, hence most long flat areas appeared as plateaus.

(d) During the crack growth stages described in (b) and (c), the crack became wider as it became longer. By the end of the stage (c), the width was as illustrated in (d).

(e) Corrosion processes produced hydrogen that diffused into the material, causing a new brittle region ahead of the crack.

Fig. 18 relates the fractography to the proposed mechanism. Point A corresponds to prior crack arrest. The hydrogen brittle envelope was developed around point A. Once the hydrogen concentration became critical, the crack grew from point A to point B at a random angle, producing a CIS slope. Subsequent crack propagation was across a region of high hydrogen concentration towards point C in a straight line. As the crack travelled it cuts across pearlite colonies indiscriminately, following the region of highest hydrogen concentration. At point C the hydrogen concentration fell below the critical level. As the crack propagated beyond point C it started to be arrested, coming to a stop at point D. The resulting fractography from point B to D was the flat plateau (mildly corrugated due to the pearlite colonies) from B to C, and the shallow dimpled MVC region between points C and D.

6. Conclusion

The microstructure of the metal did not affect hydrogen diffusion, crack propagation nor the fracture mechanism transition (slow subcritical crack growth to fast brittle failure). This was seen by the crack growing across grain boundaries irrespective of their orientation.

The crack propagated as a front outwardly from the crack initiation site, perpendicular to the free surface of the material. Hydrogen formed due to corrosion reactions diffused into the metal along the direction of the greatest triaxial stress; directly into the material perpendicular to the applied axial stress. Subcritical crack growth propagated once the material ahead of the crack tip had reached a critical hydrogen concentration. Once a critical crack size had been reached, the rest of the material failed by fast brittle failure.

Subcritical crack growth was thought to occur in two stages:

- In the first stage, the crack grew in a random manner within the hydrogen saturated area ahead of the crack tip.
- The second stage saw the crack turn and propagate directly into the material, following the path of greater hydrogen concentration. The crack continued until it hits the ductile region. Then the corrosion process continued, producing more hydrogen that diffused into the metal matrix.

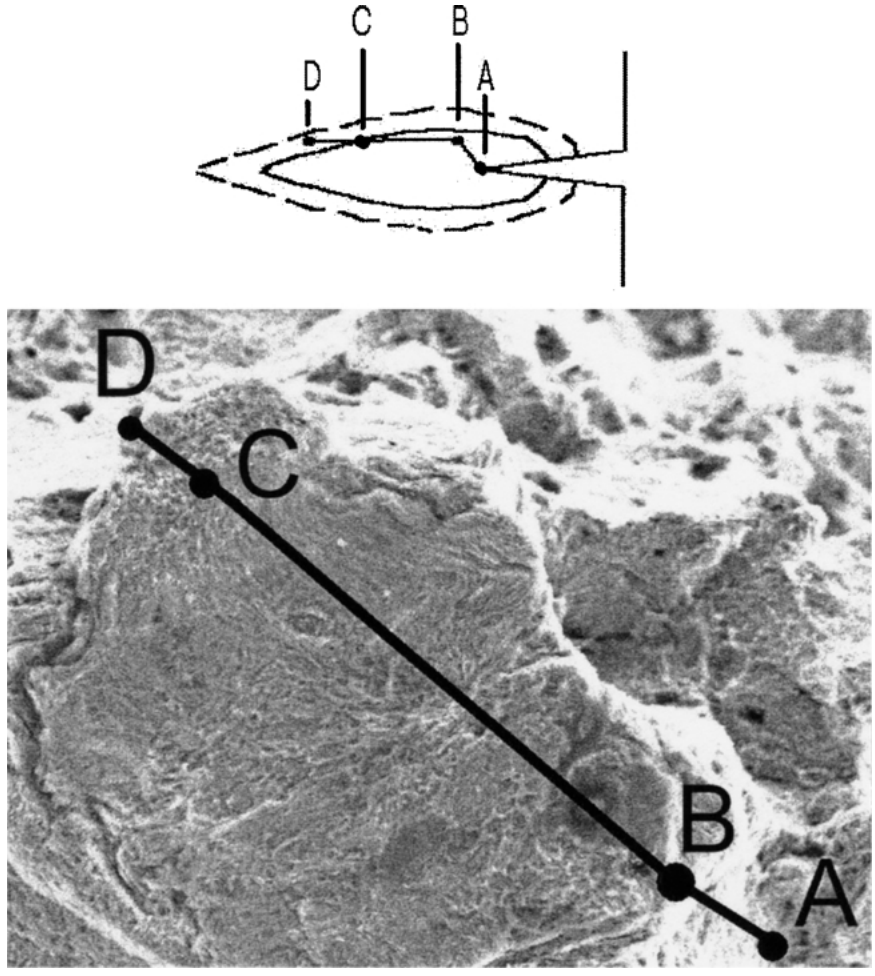

Figure 18 Crack path related to microstructure.

All this evidence suggested that the crack growth rate was dictated by the rate of hydrogen evolution at the crack tip and its rate of diffusion ahead of the crack tip.

Acknowledgements

This research is funded by an ARC SPIRT grant sponsored by Arnall Mining Products Division, Dywidag Systems international Pty Ltd.

References

1. ANI Arnall, Practical Guide to Rock Bolting, 1991, ANI ARNALL, 25 Pacific Highway Bennets Green, NSW 2290.
2. E. GAMBOA and A. ATRENS, Analysis of a Rock Bolt Failed in Service, Proceedings, 15th International Corrosion Conference, Ganada (Spain), 2002, paper 811, p. 1.
3. E. GAMBOA and A. ATRENS, Relationship of Laboratory Tests of Rock Bolt SCC to Service Failures, Proceedings, International Conference on Hydrogen Effects on Materials Behaviour and Corrosion Deformation Interactions, Wyoming (USA), September 2002.
4. J. TORIBIO and E. VASSEUR, *J. Mater. Sci. Lett.*, **16** (1997) 1345.
5. E. GAMBOA and A. ATRENS, Environmental Influence on the Stress Corrosion Cracking of Rock Bolts, Engineering Failure Analysis, 2003.
6. A. ATRENS, C. BROSNAN, S. RAMAMURTHY, A. OEHLERT and I. SMITH, *Measurement Science Technology* **4** (1993) 1281.

Received 11 September 2002
and accepted 20 May 2003